Journal of Korean Society of
Coastal and Ocean Engineers
Vol. 9, No. 4, pp. 165~175, December 1997

Deformation Characteristics of Steel Plate Cellular Bulkhead
鋼板셀 護岸의 變形特性

Jeong-Wook Jang*
張 晶 旭*

Abstract □ This study qualitatively reviewed effect of the height of loading and the ratio of penetration on the characteristics of deformation of cellular bulkhead by performing a model test of embedded steel plate cellular bulkhead which had different loading height and penetration ratio. And we also examined the effect of the loading height upon the shear behavior by performing two-dimensional model test making use of aluminum rods for a filler. Besides, test results and theoretical values based on Hansen's earth pressure theory were compared and reviewed. In consequence, it was ascertained that the yield moment of cells depended on the height of loading and the ratio of penetration, and the slip surface was located on the lower area of a cell interior according as the height of loading becomes lower. The theoretical consideration which was based on the theory of earth pressure proposed by Hansen revealed that the test results accorded with the theoretical values to some degree, and the same results were derived about the location change of the slip surface.

Keywords : cellular bulkhead, model test, shear behavior, slip surface, loading height, penetration ratio

要 旨 : 본 연구에서는 재하높이와 근입비를 달리하는 근입식 강판셀의 모형실험을 실시하여 셀 구조물의 변형특성에 미치는 재하높이와 근입비의 영향을 정성적으로 검토하였다. 또한, 채움재로 알루미늄 봉을 이용한 2차원 모형실험을 수행하여 채움재의 전단거동에 미치는 재하높이의 영향을 검토하고, Hansen의 토압이론에 근거하여 실험치와 이론치를 비교 · 검토하였다. 그 결과, 재하높이와 근입비에 따라 셀의 항복모멘트가 달라진다는 사실을 확인할 수 있었으며, 활동면은 재하높이가 낮아짐에 따라 셀 내부의 보다 낮은 곳에 위치함을 알 수 있었다. 그리고 Hansen의 토압이론에 의하여 이론적인 고찰을 수행한 결과, 실험치와 이론치는 비교적 잘 일치하였으며, 재하높이에 따른 활동면의 위치변화에 대해서는 동일한 결과를 얻었다.

핵심용어 : 셀호안, 모형실험, 전단거동, 활동면, 재하높이, 근입비

1. INTRODUCTION

A cellular bulkhead was at first used for harbour construction work which was named Black Rock near Buffallo in New York and after then it has been utilized and developed as a temporary structure for gates and cofferdam and the like. Thanks to the brilliant watertightness, self-reliance of the cellular bulkhead, the merit that relatively simple structure of it is appropriate for rapid construction, and application, it is widely put to use as a permanent structure for quaywalls and bank protections now. Recently it attracts much attention right after high appreciation of cellular bulkhead's watertightness as means of treating industrial wastes and blocking organic clays of the seabed including various kinds of detrimental materials.

Recently the cellular bulkhead has been frequently used for various harbour construction works in Korea. During construction of No.4 abandonment site executed by POSCO(Pohang iron & Steel Co. Ltd), for example,

*청주대학교 자원공학과 (Department of Mineral and Mining Engineering, Chongju University, Chongju 360-764, Korea)

the cellular bulkhead was used for bank protection on August, 1995. In addition, it was used for temporary cofferdam during construction of Seohae Grand Bridge. But there are few studies on cellular bulkhead in Korea.

During the process of moving from a cellular bulkhead as a temporary structure at the beginning to the one as a permanent structure, forms and ways of construction become diverse. The former design theories, however, do not fully meet the changes in forms and ways of construction of a cellular bulkhead. Therefore, profound research on a destruction phenomenon of cell satisfying the changed configuration of a cellular bulkhead is needed with a view to designing a cellular bulkhead as a permanent structure much more economically and safely.

The former design theories of a cellular bulkhead can be broadly divided into three classes according as how we postulate a shear face which is produced at the inside of fillers when cell is under a deformation caused by external force. In other words, they are research which assumed a vertical shear face done by from Pennoyer (1934) through Terzaghi (1945), Krynine (1945), and Tateishi (1955), the one assuming a horizontal shear face by Cummings (1957), Kitazima (1962), and the one assuming a circular shear face by Schneebeli (1957), Brinch (1953). These studies could account for many problems of a cellular bulkhead.

However, these theories have developed for sheet pile cellular bulkhead and double sheet pile wall produced as a temporary structure, and there are few studies on steel plate cellular bulkhead and embedded steel plate cellular bulkhead as a permanent structure. As Fig. 1(a) shows, the former design of cellular bulkhead which was derived from three theories above can be justified under the following concept - it is feasible when cell's resisting moment to external moment M has safety factor to certain degree. In this case, it means that if P_1h_1, P_2h_2, P_3h_3 in Fig. 1(b) are constant, the resisting moment of cell is also constant regardless of the loading height. Now, one question arises; whether the resisting moment of cell remains to be constant and invariant even when a loading height

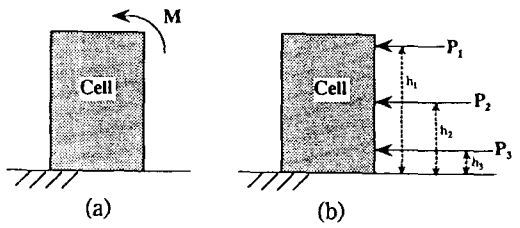

Fig. 1. Definition sketch of cellulan bulkhead.

changes into h_1, h_2, and to h_3. Little research has refered to the effects of the loading height on characteristic of deformation of cell so far. And even the former design methods were proposed to treat the cell which did not contain a penetration ratio. In other words, because it is suggested to handel a cellular bulkhead which is built on the rock, there are not sufficient studies on characteristic of deformation in proportion to the depth of penetration, in the case of embedded steel plate cellular bulkhead.

Accordingly, by investigating respective effects made on a yield load and a yield moment through the model test of stress- controlled technique, we would review the impacts of a loading height and penetration ratio on characteristic of deformation of cell. And also we would review the impacts of a loading height on the filler's shear behavior by simulating the failure-mechanism which is taking place in the filler when the external force is imflicted on the cell by the two-dimensional model test making use of aluminum rods as the fillers. In addition, this study compares and reviews the results of test and results of analysis based on Hansen's theory of earth pressure.

2. MODEL TEST OF STEEL PLATE CELLULAR BULKHEAD

2.1 Test Outline and Apparatus

By using three classes of embedded steel plate cellular bulkhead which have the different ratio of penetration, the horizontal loading test of stress-controlled technique was performed. The heights of loading are respectively top level, middle level, and bottom level.

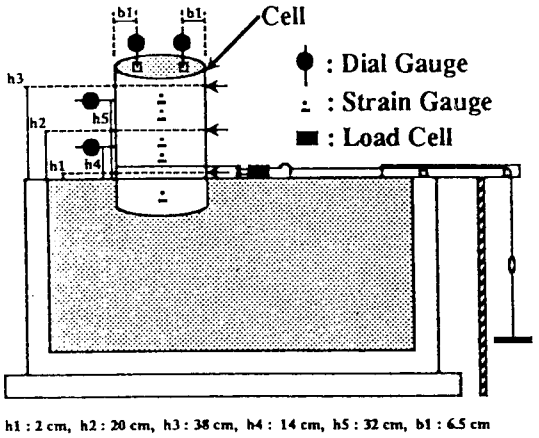

Fig. 2. Total outline of model tester.

Fig. 2 indicates the total outline of model tester and Fig. 3 shows the size of the model cell. The tester consists of a model cell, the loading apparatus and the rectangular container packed with dry sand. As the fillers and the ground material, we made the river sands of average grain diameter 1.46 mm, and uniformity coefficient 2.18 dry and tried to keep the fillers equally by dividing and hardening them into three layers. The average unit weight of fillers is γ=1.72 g/cm^3 and the unit weight of ground is γ=1.736 g/cm^3.

The way of inflicting the load is following: at first you install a stainless band with 126.8 cm in length, 4 cm in width, 0.1 mm in thickness on the model cell tightly so as to link the band and load cell, and then interlink the load cell and load plate with the help of the wire. Eventually the load is pressed over the load plate. The load is measured by the load cell and the load point is set up as 2 cm (bottom level), 20 cm (middle level) and 38 cm (top level) from the ground respectively according to heights of loading. The loading is performed step by step. When the displacement of the cell becomes stable, both of the load applied on the cell and the vertical, horizontal displacement of the cell are measured on each stage. Additionally stress change of the vertical and horizontal direction is measured as well on a respective stage by installing the strain guage vertically and horizontally on the front, back, and flank side.

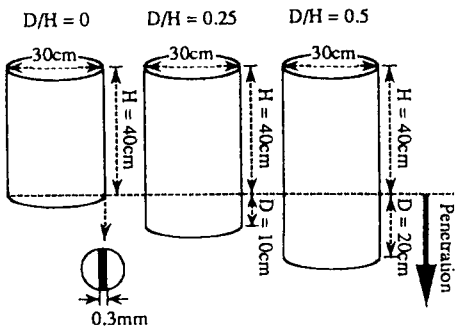

Fig. 3. Size of model cell.

2.2 Test Results

2.2.1 The definition of yield load and yield moment

You can get a bend point if you represent the relation of the Load and the displacement of the upper cell on the both logarithm graph and bridge each relation in a straight line. This bend point occurs when the change ratio of displacement of cell is salient. Therefore, this bend point is considered as apparent yield point of cell, and the load of this point is defined as the yield load, and the multiple of yield load and the loading height is defined as yield moment. Fig. 4 is one example for the way to get yield load.

2.2.2 The relation with external moment and horizontal displacement

The relation with external moment and horizontal

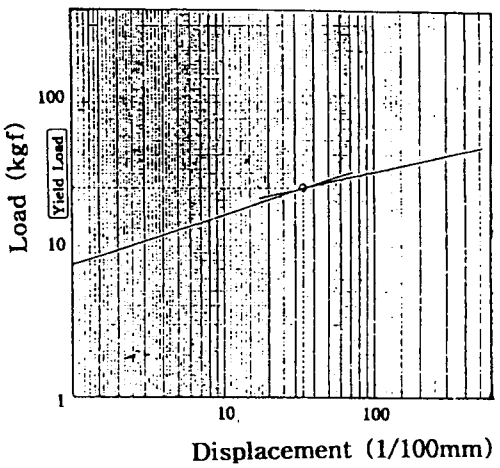

Fig. 4. One example for the way get yield load.

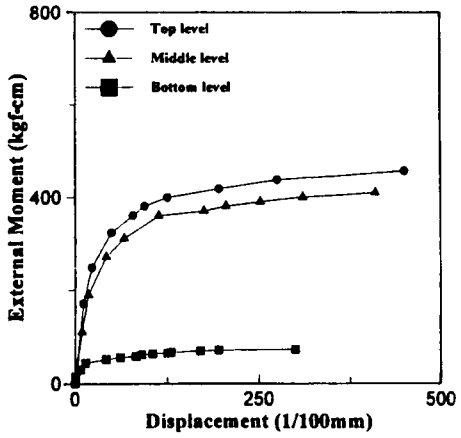

(a) D/H = 0.00

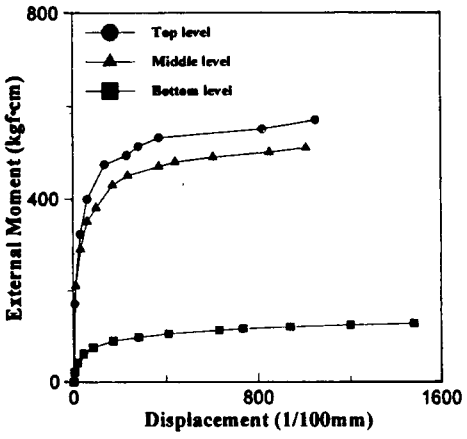

(b) D/H = 0.25

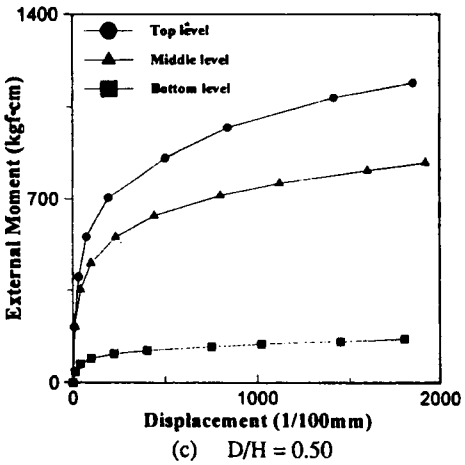

(c) D/H = 0.50

Fig. 5. Relation with external mement and horizontal displacement according to the loading height.

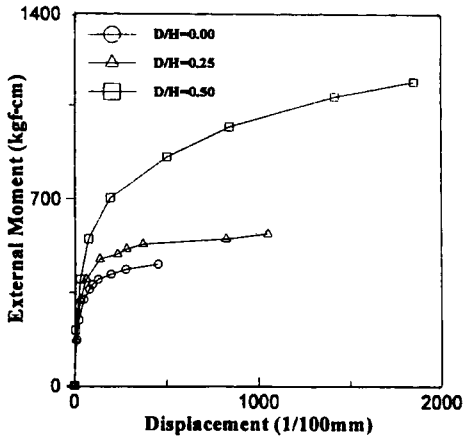

(a) Top level

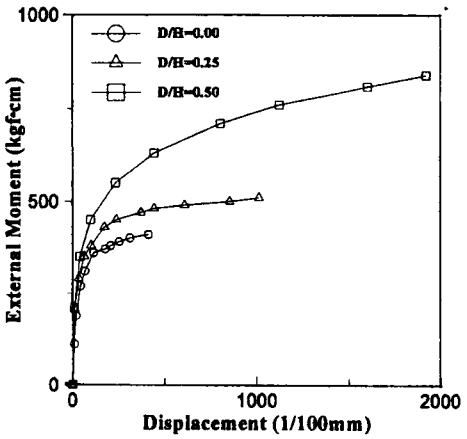

(b) Middle level

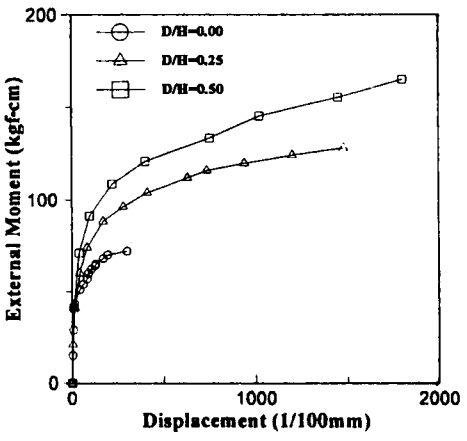

(c) Bottom level

Fig. 6. Relation with external moment and horizontal displacement according to the penetration ratio.

displacement of the cell's upper part is arranged in Figs. 5 and 6 under the condition that the height of loading and the ratio of penetration are given differently. From this figure, we can be aware the following facts; the

external moment which reaches the peak becomes smaller according as the height of loading comes to lower, and the ratio of penetration comes to smaller. Especially, the external moment which reaches the peak is a slight value in the case of loading of the bottom level compared with loading of the top level and the middle level. And we can make sure that there are many dissimilarities in the displacement amounts of the cell's upper part on the identical external moment according to the height of loading and the ratio of penetration. In other words, we can see that the displacement on the identical external moment becomes smaller according as the height of loading becomes lower and the ratio of penetration becomes larger.

2.2.3 Yield load

The yield load of each test under the condition that loading height and penetration ratio are given differently is settled in Fig. 7. This figure says that the lower loading height gets the larger yield load in the case of same penetration ratio. And in the case of same loading height, the yield load shows a tendency to increase in proportion as the peneteration ratio is growing. Especially as to the loading of bottom level, the increment of the yield load in proportion to increment of penetration ratio is considerably salient compared with the load test of variant height. The behavior of model cell by loading is broadly divided into two parts -rotation ingredient and parallel movement ingredient-. It is deduced that while the ratio of rotation ingredient is high in the top level of loading, the ratio of parallel movement ingredient is high in the bottom level of loading. Therefore, it is thought that the passive earth pressure by the parellel movement of the cell contribute to the growth of the yield load in proportion to the growth of penetration ratio in the case of the bottom level of the loading.

2.2.4 Yield moment

The yield moment of each test is arranged in Fig. 8 under the condition that loading height and penetration ratio are given differently. As with the equal ratio of peneteration, in general, the lower height of loading gets the smaller yield moment. And as with the equal height of loading, the higher ratio of penetration gets the larger yield moment. While the top level loading and the middle level loading show comparatively similar results in the case of D/H=0 and D/H=0.25, the yield moment of top level loading is larger than the one of middle level loading when D/H is 0.5. And as to the bottom level of loading, it

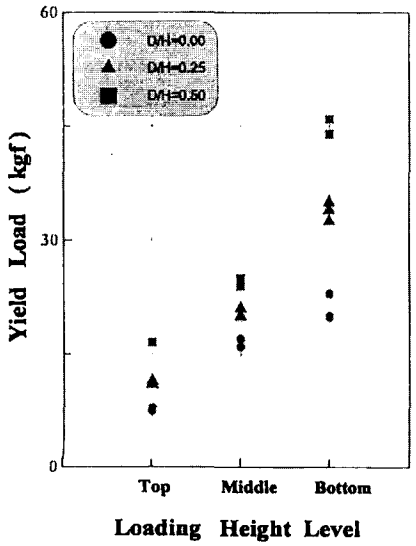

Fig. 7. Yield Load~Loading height and penetration ratio.

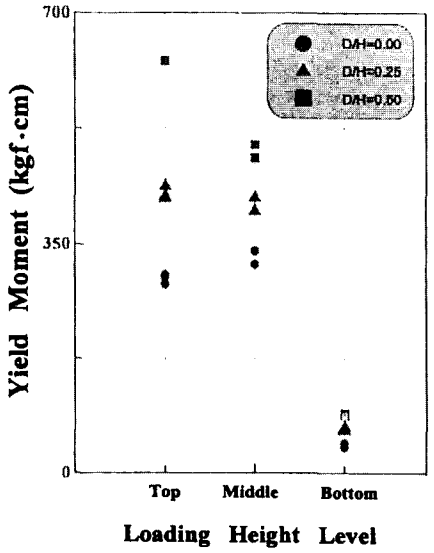

Fig. 8. Yield Moment~Loading height and penetration ratio.

shows very small results regardless of the peneration ratio.

3. TWO-DIMENTIONAL MODEL TEST

3.1 Outline of Test

Fig. 9 indicates the entire outline of two-dimensional model tester. A cell model is a structure with a highly rigid structure, being a box shaped model which is made of 0.3 mm thick steel plate to the direction of loading, and 10 mm acryl plate to the direction of section. The position of loading and the installment position of displacement device are reinforced with wood and are gone through the process of two-dimentional deformation. Because of realistic condition, two kinds of aluminium rods -Φ2 mm and Φ3 mm- are blended for the fillers and the average density is 2.15 g/cm^2. For the foundation ground, the same aluminum rods as was used for the cell fillers fill up the rectangular container made up with acryl plates of 10 mm in thickness and steel plates of 5 mm in thickness. The penetration depth of a cell model is 10 cm and the height of loading is respectively top, middle and bottom level. With the help of srain-controlled techn-ique, the loading is executed by steel-made rods which is set up at reversible-motor, and a roller is equipped in the top level of the loading rod in order not to restrain the rotation of the model.

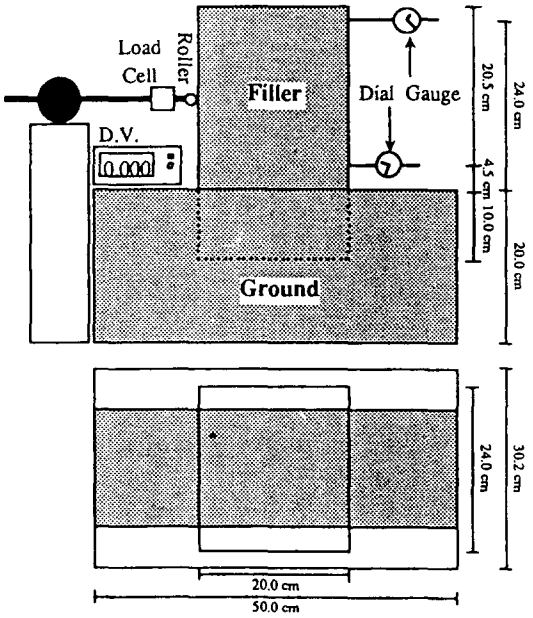

Fig. 9. Total outline of two-dimensional model tester.

The load applied to cell and the displacement amounts of cell are measured. Simultaneously, the occurence position of the slip surface and its configuration are also thought over by reporting the filler's movement with the photograph and the video.

3.2 Test Results

3.2.1 Maximum load and maximum moment

Table 1 shows the test condition, the maximum load of each test, and the moment of the point where it comes up to the peak when the height of loading is given differently. The height of loading which is shown in that table starts from the ground level.

From Table 1, we can be aware that as the height of loading becomes lower, the maximum load becomes

Table 1. Test condition and test result.

Test No.	Loading Height (cm)	Density of Ground (g/cm^3)	Density of Filler (g/cm^3)	Maximum Load (kgf)	Maximum Moment (kgf·cm)
TEST1	24.6	2.16	2.15	5.58	139.7
TEST5	24.6	2.15	2.16	5.95	146.4
TEST7	24.6	2.14	2.16	5.99	147.4
TEST2	12.4	2.19	2.16	8,57	106.3
TEST6	12.9	2.17	2.16	9.55	128.5
TEST9	12.0	2.19	2.14	9.26	111.1
TEST3	5.1	2.15	2.16	13.77	70.2
TEST4	5.5	2.16	2.12	13.34	78.5
TEST8	5.5	2.15	2.21	14.03	77.6

higher, and the maximum mement becomes lower inversely. This result coincides with that of model test of steel plate cell and we can re-identify the influence of the loading height on the filler's shear behavior from this fact.

3.2.2 Distribution of displacement and strain

Fig. 10 shows a displacement distribution chart of the fillers. This figure is based on the displacement of

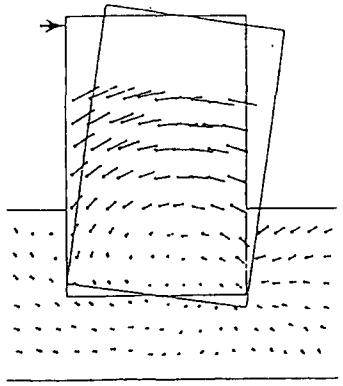

(a) TEST 1

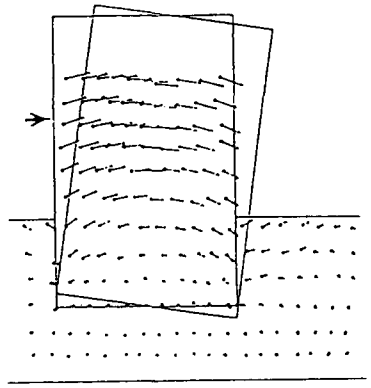

(b) TEST 9

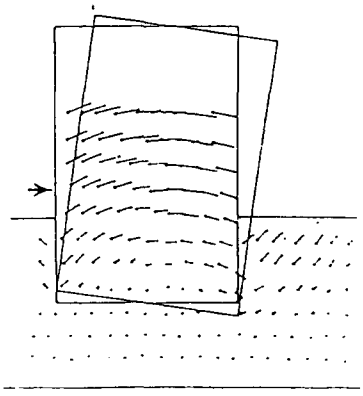

(c) TEST 4

Fig. 10. Distribution of displacement.

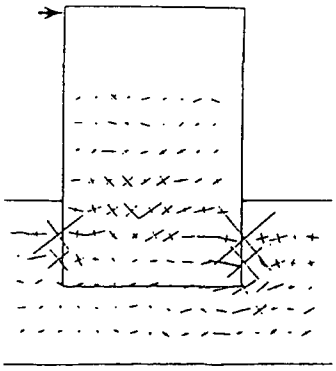

(a) TEST 1

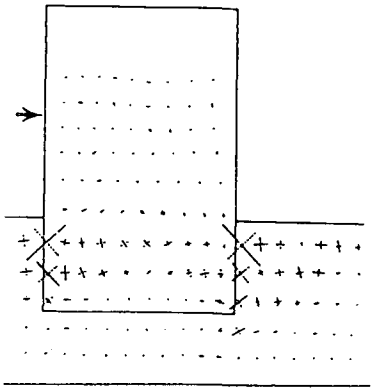

(b) TEST 9

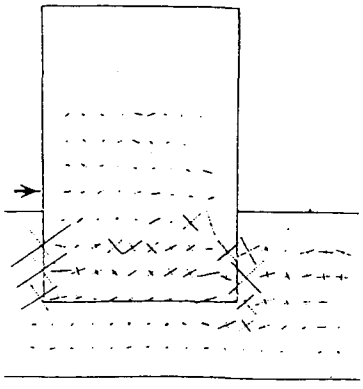

(c) TEST 4

Fig. 11. Distribution of strain.

aluminum rods between the prior of loading and the posterior of loading, which was marked on the stage of test preparation. Fig. 11 is a strain distribution chart which is derived from the displacement distribution chart in Fig. 10.

In this figure, two straight lines which intersect vertically each other indicates the maximum principal strain and the minimum principal strain at the intersect point. A dotted line means a compressive strain and a solid line means a tensile strain.

As the loading is proceeding, the slip takes place little by little in the aluminum rods of the fillers, which leads to divide into two parts-one part has a large displacement, and the other has a small one. Fig. 10 shows the boundary surface of the large displacement and the small displacement. And it is also observed from Fig. 11 that the part which has apparently high strain is making a line compared with the around part. This fact proves that its position and configuration usually tend to coincide with each other compared with the boundary surface of displacement distribution chart in Fig. 10. Some temporary conclusions are derived from these facts that this boundary surface corresponds to the slip surface and it lies in the lower position of the cell interior as the height of loading gets lower.

Even though it is not easy to presume the configuration of the slip surface objectively, we can be aware that it has remarkable similarity to circular failure face supposed by Schneebeli or Hansen rather than vertical failure face supposed by Terzaghi and a horizontal failure face assumed by Cummings and so on. And also it is discernable that there exist somewhat difference in the configuration of the slip surface according to the height of loading.

It seems that the alteration in the configuration of the slip surface and the occurrence position in proportion to the height loading have its origin in the difference of the passive earth pressure of penetration parts located in the non-loading sites. And the differentiation of maximum load and maximum moment in proportion to the height of loading is ascribed to the alteration in the configuration and the occurrence position of the slip surface.

3.2.3 Theoretical survey

3.2.3.1 Hansen's earth pressure theory

Hansen's earth pressure theory is the method that works out the ultimate horizontal resist force of the cellular bulkhead from the equillibrium relation of each force by supposing the circular slip face crossing the tail end of the cell. Fig. 12 shows the equillibrium of force in two-dimensional model test. We can induce equations as following by applying the equillibrium equation of force.

$$Q = H - E_1 + E_2 \tag{1}$$

$$\gamma_w \mathrm{wh} + G - V - F_1 - F_2 = 0 \tag{2}$$

$$M_R + Q_q + \frac{1}{2}\mathrm{w}(F_1 - F_2) + E_1 z_1 - E_2 z_2 = 0 \tag{3}$$

where G is the weight of the volume included between the tail end surface of the cell and the slip surface. G and reaction force are induced by the following equations.

$$G = \gamma \mathrm{w}^2 G^{\gamma z}$$

$$V = \gamma \mathrm{w}^2 (V^{\gamma z} + V^{\gamma x} \sin 2\phi) - cw \cot\phi + w\, V^{ty} \left(t' + \frac{c}{\sin\phi}\right) \tag{5}$$

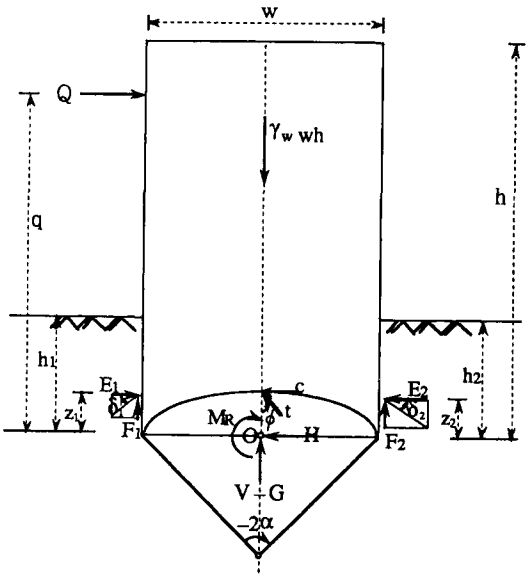

Fig. 12. Equilibrium of force in two-dimensional model test.

$$H = \gamma w^2 (H^{\gamma z} + H^{\gamma\gamma} \cos 2\phi) + wH^{ty} \left(t' + \frac{c}{\sin\phi} \right) \quad (6)$$

$$M_R = \gamma w^3 M_R^{\gamma\gamma} + w^2 M_R^t \left(t' + \frac{c}{\sin\phi} \right) \quad (7)$$

where γ is the unit weight of the filler near the slip surface, and c is the cohesion of the filler. We can get the following equations by substituting Eqs. (4)~(7) into Eqs. (1)~(3) and rearranging them.

$$Q = \gamma w^2 D \left(G^{\gamma z} - V^{\gamma} + H^{\gamma} \frac{1}{D} \right) + \gamma_m wh D - F_1 D + F_2 D + E_2 - E_1 \quad (8)$$

$$t' = \frac{(\gamma_m h + \gamma w G^{\gamma z} - \gamma w V^{\gamma} - \frac{F_1 + F_2}{w})}{V^{ty}} \quad (9)$$

$$\gamma w^3 M_R^{\gamma\gamma} + t' w^2 M_r^t + Q_q + \frac{w(F_1 - F_2)}{2} + E_1 z_1 - E_2 z_2 = 0 \quad (10)$$

wherein γ_m is the average unit weight of the filler.

$$V^{\gamma} = V^{\gamma z} + V^{\gamma\alpha} \sin 2\phi$$

$$H^{\gamma} = H^{\gamma z} + H^{\gamma\gamma} \cos 2\phi$$

$$D = H^{ty} / V^{ty}$$

$$E_1 = \frac{1}{2} \gamma h_1^2 \lambda_r^a \quad F_1 = E_1 \tan\delta_1$$

$$E_2 = \frac{1}{2} \gamma h_2^2 \lambda_r^p \quad F_2 = E_2 \tan\delta_2$$

$$\lambda_r^p = \rho_r + 0.007 (e^{9\sin\phi} - 1)$$

$$\rho_r^p = e^{\mu(\pi/2+\phi)} \cos\phi \tan\left(45^o + \frac{\phi}{2} \right) \quad (\mu = \tan\psi)$$

In addition, each coefficient which is the function of α can be drawn through the equations as following.

$$G^{\gamma z} = \frac{1}{4} (\alpha + \alpha \cot^2\alpha - \cot\alpha)$$

$$M_R^{\gamma\gamma} = \cos\psi \frac{\cot\alpha}{16\sin^2\alpha} (A + B)$$

$$A = 2\alpha \sin\psi + 4\sin\phi \cos(\psi + \phi) \tan\alpha - \cos 2\phi \cos(\psi - 2\alpha)$$

$$B = -\cos\psi \cos 2\psi + \cos(\psi + \phi + \alpha)$$

$$\{2\nu \cos\psi \cos(\psi - \phi + \alpha) - (\nu - 1)\cos\phi \sec\alpha\}$$

$$\tan\psi = 2\tan\phi$$

$$\nu = e^{4\mu\alpha}$$

$$M_R^t = \frac{\cos\psi \cot\alpha}{4\sin\alpha} \{\cos(\psi - \phi + \alpha) - \nu \cos(\psi - \phi + \alpha) + \frac{1}{2}(\nu - 1)\cos\phi \sec\psi \sec\alpha\}$$

$$V^{z\alpha} = \frac{\cos^2\psi}{8\sin^2\alpha} \{\sin 2\psi - \nu \sin(2\psi + 2\alpha) + 2\alpha\}$$

$$V^{\alpha z} = -H^{\gamma\gamma} = \frac{\cos^2\psi}{8\sin^2\alpha} \{\nu - \sec\psi \cos(\psi - 2\alpha)\}$$

$$H^{z\alpha} = \frac{\cos^2\psi}{8\sin^2\alpha} \{\cos 2\psi - \nu \cos(2\psi + 2\alpha) - 2\alpha \tan\psi\}$$

$$H^{ty} = -V^{\alpha\alpha} = \frac{\cos\psi}{2\sin\alpha} \{\nu \cos(\psi - \phi + \alpha) - \cos(\psi - \phi - \alpha)\}$$

$$V^{ty} = -H^{\alpha} = \frac{\cos\psi}{2\sin\alpha} \{\nu \sin(\psi - \phi + \alpha) - \sin(\psi - \phi - \alpha)\}$$

Therefore if we insert values of the angel of internal friction, ϕ and α, we can get values of each coefficient, and if we apply these values to Eq. (8) and Eq. (9), we can get values of Q and t'. We can ascertain the satisfaction of Eq. (8) by inserting Q and t' drawn as such to Eq. (10). If we cannot satisfy Eq. (10), repeat the calculation changing the value of α until the equation is satisfied. Q that satisfies Eq. (10) becomes the ultimate horizontal resist force, and the value of α at that time determines the position of the slip surface.

3.2.3.2 Comparision of calculation results and test results

Ultimate horizontal resist force has been induced from the two-dimensional model test performed in study based on Hasen's earth pressure theory. During performing the calculation, We made following hypothesis.

1) As the aluminum rod has been used as the filler, the cohesion of the filler is regarded as almost nonexistent, and c=0 has been led.

2) We fixed $\delta_1 = \delta_2 = \phi$. Here, as the value of ϕ of aluminum rod used as the filler is ϕ=24 which is the result of the test using the triaxial compression tester, we used that value.

3) We neglected the ground reaction forces E_1, F_1 (active earth pressure) of the loading side regarding them as the minute values.

Table 2 arranges the maximum load of each test, the ultimate horizontal resist force which is from calculation and α in that case corresponding to each loading height. The height of loading in Table 2 is the one from the bottom surface of cell.

Table 2. Comparison between test results and calculation results.

Test No.	Loading Height (m)	Maximum Load (Experiment) (kgf)	Ultimate horizontal resisting force (kgf)	α (degree)
Test 1	0.35	5.58	5.40	-84
Test 5	0.35	5.95	5.43	-84
Test 7	0.34	5.99	5.32	-81
Test 2	0.23	8.57	8.24	-75
Test 6	0.23	9.55	8.43	-75
Test 9	0.23	9.26	8.22	-73
Test 3	0.16	13.77	11.40	-60
Test 4	0.16	13.34	11.47	-62
Test 8	0.16	14.03	11.24	-61

We can see from this table that the ultimate horizontal resisting force varies a little between test results and calculation results in case of the test with low loading heights, but shows a considerable consistency in the other test. In addition to that, as for the loading height and central angle α of the circular slip surface, we can see that, just as results of test, the lower heights gets the lower the position of the slip surface.

4. CONCLUSIONS

Through the stress-controlled technique, the horizontal loading test that had the different loading height and the penetration ratio was performed and each effect on characteristic of deformation of cells was qualitatively analysis reviewed by examining the effects of the peneteration ratio and the loading height on the yield load and the yield moment. On consequence, we could arrive at some conclusion.

1) Concerning the equal ratio of penetration, the yield load becomes larger and yield moment shows a slight value invertedly and the displacement on the identical external moment becomes smaller according as the loading height becomes lower. Especially, the yield moment is a very slight value in the case of the loading of bottom level compared with the loading of top level and the middle level.

2) Concerning the equal height of loading, the yield load and the yield moment shows the lager values and the displacement on the identical external moment becomes smaller according as the ratio of penetration becomes higher. The effects of the penetration ratio on the stability of the cell come to grow especially in the case of bottom loading level.

3) Even though the stress changes of the cell were measured with a view to examining the influences of the loading height and the penetration ratio on the stress of the cells, the stress distribution showed the very complicate configuration because the steel plate of the cell was thin. So few tendency was observed.

4) It was ascertained the yield moment depends on the height of loading and the ratio of penetration. Therefore, something a little bit illegitimate exists in the former design method because it did not take into account the height of loading.

Concerning the embedded cellular bulkhead, additionally, we performed the two-dimentional model test using the aluminum rods and examined the failure mechanism arising in the interior of the fillers. And also after examining the effects of the loading heights on the shear behavior of the fillers, we were able to get to some conclusions.

5) As the height of loading becomes lower, the maximum load that the cell can withstand becomes larger, but the maximum moment becomes smaller invertedly. This result corresponds to one of the model test of steel plate cellular bulkhead, which leads to confirm the loading height's effects on the characteristic of deformation of the cell.

6) We could identify the bounding surface which was regarded as sliping surface. This boundary surface is located on the lower area of the internal according as

the height of loading becomes lower. Besides, though the configuration of the slip surface was not objectively estimated with high accuracy, we can reason that it is a little bit similar to the circular failure surface suggested by Schneebeli.

7) The theoretical consideration based on the theory of earth pressure proposed by Hansel revealed that the test results accorded with the theoretical value to a degree. About the location changes of the slip surface, the same results were derived.

8) Because this test focused on the equal depth of penetration, we know little about the configuration changes of the slip surface in proportion to the ratio of penetration. This still remains to be demonstrated henceforward.

9) It is deducible that changes of the maxium load and the maxium moment according to the loading height result from changes of the configuration of the slip surface and its occurrence position according to the loading height.

The qualitatively analysis results of two tests above make sure that it is the height of the loading and ratio of penetration that give the foremost influence on the characteristic of deformation of the cell. With due regard to the height of loading and the ratio of penetration, the further studies on the quantative interpretation about two effective elements and the design method of the cellular bulkhead are sorely needed.

REFERENCES

Cummings, E.M., 1957. Cellular cofferdams and docks, ASCE *Proc.* WW3, Sept.

Cummings, E.M., 1960. Cellular cofferdam and docks, *Transaction*, ASCE, Vol. 125.

Brinch, J. and Hansen, J.B., 1953. Earth pressure calculation, *The Danish Technical Press*, The Insitution of Danish Civil Engineers, Copenhagen.

Ishiguro, K., Shiraishi, M. and Umiwa, H., 1968. Steel sheet pile construction, Sankaido (in Japanese).

Jang, J.W., 1993. Studies on horizontal behavior of cellular bulkhead, *Doctoral thesis submitted to Univ. of Tsukuba* (in Japanese).

Jang, J.W., Sawaguchi, M. and Yamada, Y., 1993. Model test with aluminium rods on shear behavior of fill in cellular bulkhead, *Proc. 27th Japan National Conf. on Soil Mech. and Found.* (in Japanese).

Kitajima, S., 1962. Failure of cellular bulkhead on rock, *Soil Mech. and Found. Eng.*, **10**(8) (in Japanese).

Krynine, D.P., 1945. Discussion on stability and stiffness of cellular cofferdams, *Transaction*, ASCE, Vol. 110.

Schneebeli, C., 1957. Contribution au calcul de la stability des batardeaux a double paroi de palplanches, *Proc.* 4th I.C.S.M.F.E., Aug.

Tateishi., T., 1955. Design method of cellular bulkhead, *Soil Mech. and Found. Eng.*, **3**(9) (in Japanese).

Terzaghi, K., 1945. Stability and stiffness of cellular cofferdam, *Transaction*, ASCE, Vol. 110.